This is the accepted manuscript made available via CHORUS. The article has been published as:

Description of ^{158}Er at ultrahigh spin in nuclear density functional theory

A. V. Afanasjev, Yue Shi, and W. Nazarewicz

Phys. Rev. C **86**, 031304 — Published 17 September 2012

DOI: 10.1103/PhysRevC.86.031304

Description of ^{158}Er at ultrahigh spin in nuclear density functional theory

A. V. Afanasjev,[1,2] Yue Shi,[3] and W. Nazarewicz[4,5,6]

[1] *Department of Physics and Astronomy, Mississippi State University, Mississippi 39762, USA*
[2] *Joint Institute for Heavy-Ion Research, Oak Ridge, Tennessee 37831, USA*
[3] *State Key Laboratory of Nuclear Physics and Technology, School of Physics, Peking University, Beijing 100871, China*
[4] *Department of Physics and Astronomy, University of Tennessee, Knoxville, Tennessee 37996, USA*
[5] *Physics Division, Oak Ridge National Laboratory, Oak Ridge, Tennessee 37831, USA*
[6] *Institute of Theoretical Physics, University of Warsaw, ul. Hoża 69, PL-00-681 Warsaw, Poland*

Rotational bands in ^{158}Er at ultra-high spin have been studied in the framework of relativistic and non-relativistic nuclear density functional theories. Consistent results are obtained across the theoretical models used but some puzzles remain when confronted with experiment. Namely, the many-body configurations which provide good description of experimental transition quadrupole moments and dynamic moments of inertia require substantial increase of the spins of observed bands as compared with experimental estimates, which are still subject to large uncertainties. If, however, the theoretical spins assignments turned out to be correct, the experimental band 1 in ^{158}Er would be the highest-spin structure ever observed.

PACS numbers: 21.60.Jz, 21.10.Re, 21.10.Ky, 27.70.+q

The existence of nuclei with triaxial shape deformations has been a topic of active research since the early fifties [1, 2]. So far, there has been no clear evidence for nuclei that are triaxial in their ground states, and theoretical mass table calculations predict very few such candidates having fairly small energy gain due to triaxiality [3]. By far the clearest signatures come from the γ-ray spectroscopy of rotating nuclei since the angular momentum alignment of nucleons in high-j orbitals creates the shell structure which favors triaxiality at certain combinations of proton and neutron numbers, and specific rotational frequencies [4]. However, the evidence for existence of static triaxial shapes still remains scarce. It is generally accepted that the smooth terminating bands evolve gradually through the γ-deformation plane on approaching band termination [5]; this feature is supported by the measurements of transition quadrupole moments [6]. The rotational bands associated with the rigid triaxial shapes show specific features that allow to distinguish them from axially symmetric structures. Here, excellent examples are wobbling [7, 8] and chiral [9] bands.

Triaxial superdeformed (TSD) bands represent another class of structures built on static triaxial shapes. Of particular interest are the bands recently observed at ultrahigh spins in the $A \sim 154-160$ mass region. These are the bands seen in ^{154}Er [10], ^{157,158,159,160}Er [11–15], ^{157}Ho [12], and ^{160}Yb [16]. As discussed below, the interpretation of these structures is still under debate. The cranking calculations of Refs. [17, 18] predicted that collective triaxial configurations with large quadrupole deformations become competitive for spins above $50\hbar$. More recent cranked Nilsson-Strutinsky (CNS) analysis of potential energy surfaces at the spins of interest have revealed the existence of three local minima [19], namely, TSD1 with $\varepsilon_2 \sim 0.34$ and positive value of $\gamma \sim 20°$, TSD2 with $\varepsilon_2 \sim 0.34$ and negative value of $\gamma \sim -20°$, and TSD3 with $\varepsilon_2 \sim 0.45$ and positive value of $\gamma \sim 25°$. (For consistency with earlier publications, we adopt the CNS labeling of triaxial minima in this work. Note, however, that DFT calculations yield $\gamma-$deformations that are typically smaller in absolute value than the ones obtained in CNS.) The early interpretation of observed TSD bands have invoked configurations built either upon the TSD1 minimum [10, 11] or TSD1 and/or TSD2 minima [13].

However, the recent measurements of transition quadrupole moments of the TSD bands in ^{157,158}Er nuclei [19] ruled out – at least for these two nuclei – the interpretation based on the TSD1 minimum since the associated transition quadrupole moments of $Q_t \sim 7.5$ eb are significantly lower than the experimental values of ~ 11 eb. In addition, it was shown in the recent self-consistent tilted-axis cranking (TAC) study [20] that the excited minimum TSD2 becomes a saddle point if the rotational axis is allowed to change direction, i.e., the mere appearance of TSD2 is an artifact of one-dimensional cranking approximation. The TAC work suggested the interpretation of observed TSD bands in terms of TSD3. Such option has also been considered in the CNS calculations of Refs. [19, 21], however, no detailed study of it has been performed. On the contrary, a TSD2 scenario has been put forward in the most recent paper [21]. The goal of this manuscript is to perform the detailed analysis of the observed TSD bands within the self-consistent framework based on nuclear density functional theory (DFT).

Our calculations for ^{158}Er have been carried out within two complementary theoretical methods; namely, relativistic (covariant) DFT [22] and non-relativistic Skyrme-DFT [23]. Since the TAC analysis [20] does not indicate the presence of tilted-axis solution for the TSD3 bands, we apply the principal axis cranking approximation. Moreover, because of very large angular momenta involved, pairing correlations are neglected. The resulting schemes are referred to as the cranked relativistic

mean field (CRMF) [24] and cranked Skyrme Hartree-Fock (CSHF). In the CRMF calculations, all fermionic and bosonic states belonging to the shells up to $N_F = 14$ and $N_B = 20$ are taken into account in the diagonalization of the Dirac equation and the matrix inversion of the Klein-Gordon equations, respectively. The NL1 [25] and NL3* [26] parametrizations are used for the RMF Lagrangian; according to the recent study [27] these sets provide a reasonable description of the deformed single-particle energies. In the CSHF calculation, we use the symmetry unrestricted Hartree-Fock solver HFODD (v2.49) [28] and the SkM* energy density functional [29], which gives reasonable results in this mass region [20]. The CSHF calculation are performed in the stretched harmonic oscillator basis consisting of 680 basis states. The detailed investigations indicate that these truncation schemes provide a very reasonable numerical accuracy.

The results of the calculations for the configurations at, or slightly above, the collective yrast line, are summarized in Fig. 1. The configurations can be divided into different groups according to their triaxiality and transition quadrupole moments in the spin range of $30 - 70\hbar$. Near-prolate configurations with $|\gamma| \leq 6°$ are labeled AX. Their transition quadrupole moments are smaller than 9 eb so AX cannot be associated with the observed bands. Triaxial configurations with positive $\gamma \sim 10°$ and transition quadrupole moments $Q_t \leq 9$ eb are labeled TSD1, while TSD2 are the configurations with negative $\gamma \sim -10°$. Triaxial configurations with positive $\gamma \sim 13°$ and transition quadrupole moments $Q_t \geq 9$ eb are labeled TSD3; their single-particle content is given in Table I. As mentioned earlier, $\gamma-$deformations in DFT are usually smaller than those in CNS.

TABLE I. TSD3 configurations studied in this work. Each configuration is defined by the number of neutrons and protons occupying the four parity-signature (π, r) blocks: $[(\pi = +, r = +i), (\pi = +, r = -i), (\pi = -, r = +i), (\pi = -, r = -i)]$.

conf. label	configuration
TSD3(a)	$\nu[23, 22, 23, 22] \otimes \pi[17, 17, 17, 17]$
TSD3(b)	$\nu[23, 23, 22, 22] \otimes \pi[17, 17, 17, 17]$
TSD3(c)	$\nu[24, 22, 22, 22] \otimes \pi[17, 17, 17, 17]$
TSD3(d)	$\nu[24, 23, 22, 21] \otimes \pi[17, 17, 17, 17]$

It is rewarding to see that the general structure of near-yrast bands predicted in ^{158}Er weakly depends on the DFT model/parametrization used. However, the relative energies of the calculated configurations do depend on model/parametrization, thus reflecting the differences in the predicted energies of the single-particle states. Nevertheless, in all three models employed in our study, the configurations TSD3 approach yrast at $70\hbar$, and TSD2 always appear excited at very high spins (which rules them out [20]). It is also important to mention that the configurations belonging to the same group have similar rotational inertia (slopes) in Fig. 1.

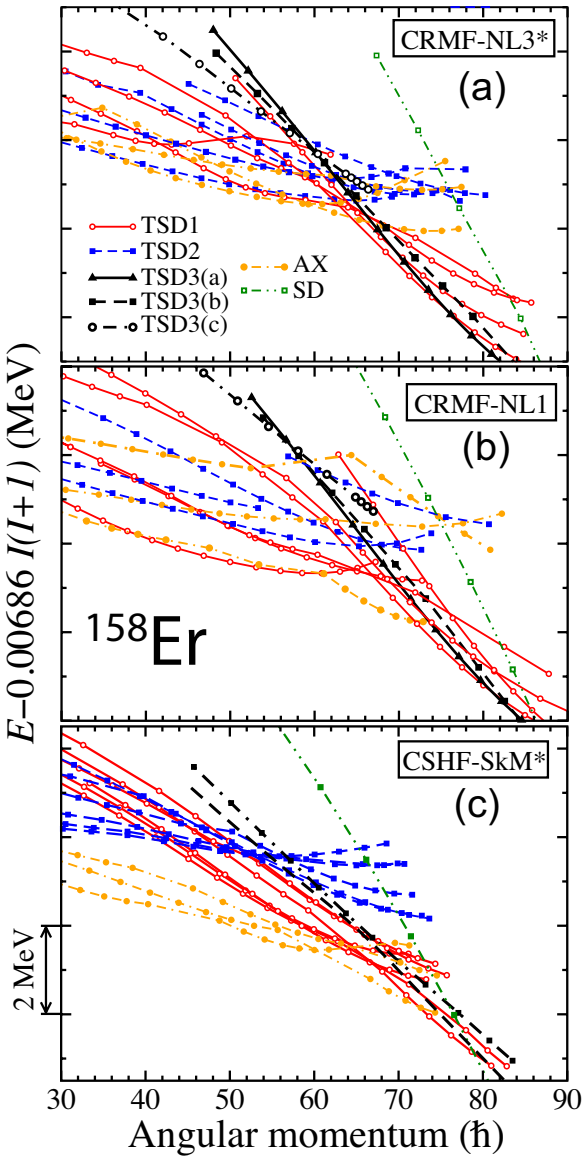

FIG. 1. (Color online) Energies of various configurations in ^{158}Er calculated in the range of $I = 30 - 90$ using (a) CRMF-NL3*, (b) CRMF-NL1, and (c) CSHF-SkM*, relative to a smooth reference $E_{RLD} = AI(I + 1)$ with the inertia parameter $A = 0.00686$ MeV. The lowest-energy near-prolate superdeformed configuration with quadrupole deformation $\beta_2 \geq 0.6$ is labeled as SD. See text for details.

The configuration TSD3(a) – involving two protons in $N = 6$ shell and one neutron in $N = 7$ shell, i.e., $\pi 6^2 \nu 7^1$ – is a possible CRMF candidate for the observed band 1. Single-particle CRMF-NL3* routhians corresponding to this configuration are shown in Fig. 2. (Similar routhians have also been obtained in CSHF.) In CRMF, the transition quadrupole moment Q_t of TSD3(a) changes from 10.5 eb at $I = 42$ to 9.0 eb at $I = 72$ and γ slightly increases from 12° to 16° in this spin range. Considering that experimental value of Q_t is subject to $\approx 15\%$ uncertainty due to nuclear and electronic stopping powers,

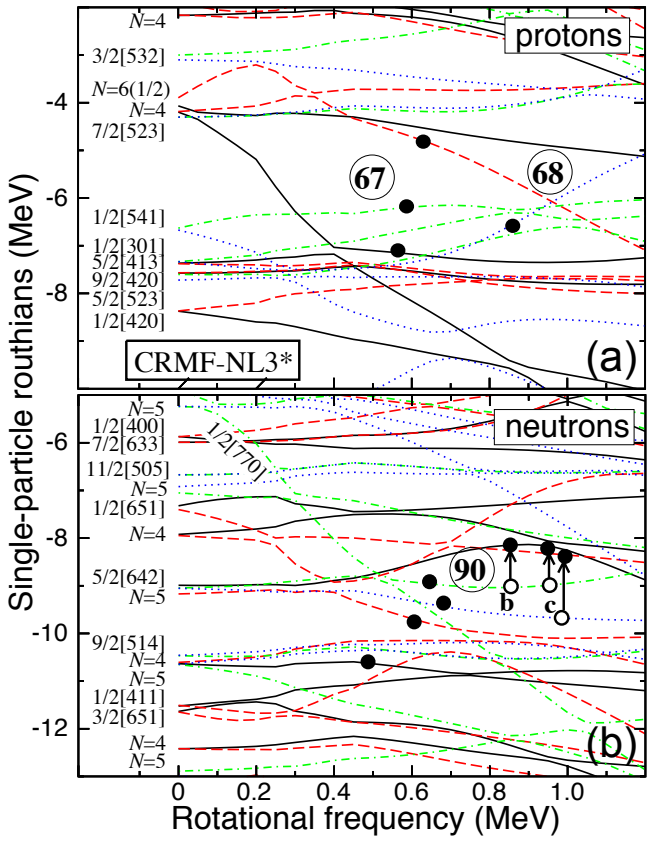

FIG. 2. (Color online) Proton (top) and neutron (bottom) single-particle routhians in CRMF-NL3* as a function of rotational frequency Ω_x. They are given along the deformation path of TSD3(a) at $\Omega_x \geq 0.45$ MeV; at lower frequencies the deformation is fixed to the one obtained at $\Omega_x = 0.45$ MeV. Levels are labeled by parity π and signature r quantum numbers. Solid, short-dashed, dot-dashed and dotted lines indicate $(\pi = +, r = -i)$, $(\pi = +, r = +i)$, $(\pi = -, r = +i)$ and $(\pi = -, r = -i)$ orbitals, respectively. At $\Omega_x = 0$ MeV, single-particle routhians are marked by means of either asymptotic quantum numbers $\Omega[Nn_z\Lambda]$ (in the case when the squared amplitude of the dominant Nilsson component is greater than 0.5) or by the dominant principal quantum number N. Solid circles indicate the last (π, r) orbitals occupied within each (π, r) family. Neutron particle-hole excitations leading to configurations TSD3(b) and TSD3(c) are marked by arrows.

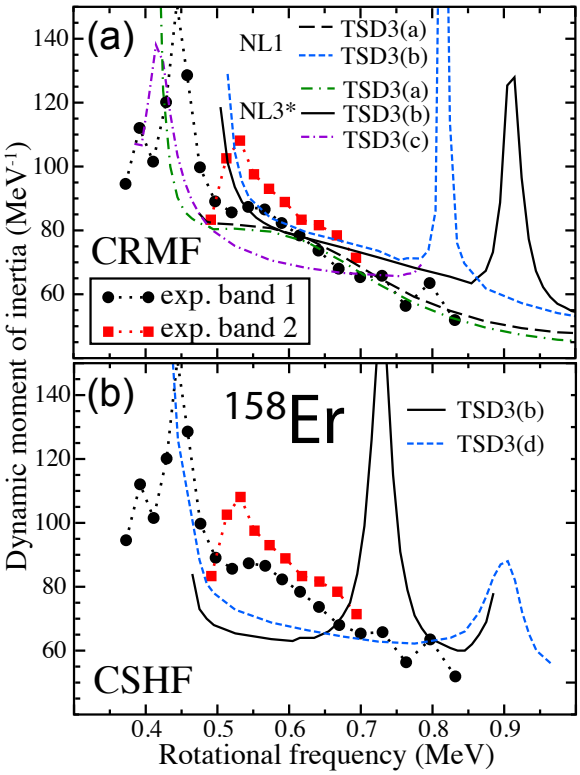

FIG. 3. (Color online) Experimental dynamic moments of inertia of observed TSD bands in ^{158}Er (symbols) compared to calculated ones (lines) in (a) CRMF and (b) CSHF. The calculated values are shown only in the frequency range in which the self-consistent solution corresponding to the band in question exist. See text for details.

these values are reasonably close to experiment. Moreover, as seen in Fig. 3(a), the experimental dynamic moment of inertia $J^{(2)}$ is rather well reproduced by assuming this configuration above the band crossing at low frequencies; the level of agreement with experiment is comparable to that earlier obtained for superdeformed bands in the $A \sim 150$ region [24, 30].

Our CRMF-NL3* calculations suggest that the jump in dynamic moment of inertia of band 1 at low frequencies (see Fig. 3) can be associated with a band crossing with large interaction between the $1/2[770](r = +i)$ and $[N = 5](r = +i)$ neutron routhians seen in Fig. 2(b). In CRMF-NL1, the interaction between these routhians is weak so it can be removed by going to the diabatic representation [5].

However, the interpretation of band 1 in terms of TSD3(a) is not consistent with the current experimental spin assignments. A high-fold analysis of the intensity profiles at the bottom of band 1 in ^{158}Er, compared to feeding intensities into the known yrast states, has allowed an estimation of the highest spin reached by this band to be $\sim 65\hbar$ [11]. At present, the uncertainty of this procedure is not obvious, however, the experimental error on spin assignment can be larger than $4\hbar$ [31]. The comparison between experimental and calculated energies shown in Fig. 4 indicates that, to be consistent with TSD3(a), band 1 has to be observed in the spin range $I = 35 - 77$. If this were the case, band 1 would be the rotational structure observed at the highest spin ever. Considering the fact that this band carries only $\sim 10^{-4}$ of the respective channel intensity, i.e., two orders of magnitude less than the superdeformed yrast band in ^{152}Dy observed up to $68\hbar$ [32], this possibility cannot be excluded.

If TSD3(a) is assigned to band 1, then the CRMF configuration TSD3(b) built upon TSD3(a) by exciting a

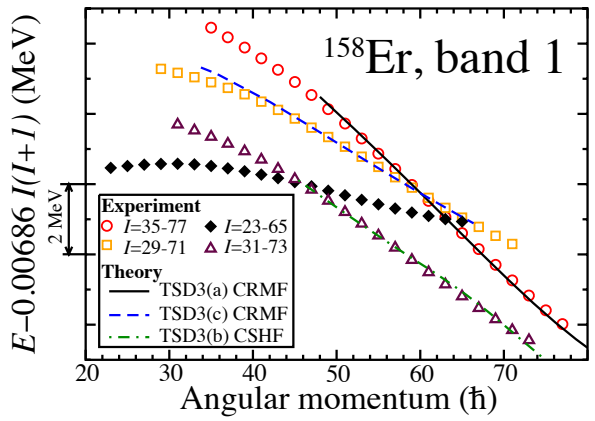

FIG. 4. (Color online) Similar as in Fig. 1 but for experimental band 1 assuming different spin assignments (symbols), and for calculated configurations TSD3(a) and TSD3(c) in CRMF-NL3*, and TSD3(b) in CSHF-SkM* (lines). The energy of the lowest experimental state is selected arbitrarily to minimize the deviation from calculated configurations.

neutron from $N = 5$ $(r = +i)$ into $5/2[642](r = -i)$ is a natural candidate for experimental band 2. Indeed, as seen in Fig. 3, $J^{(2)}$ of this configuration is close to that of band 2, and its transition quadrupole moment is only slightly larger (by ~ 0.7 eb) than that of TSD3(a). Similar to the case of TSD3(a), the increase of $J^{(2)}$ at low frequencies predicted for TSD3(b) is due to an unpaired band crossing with a strong interaction between the $\nu 1/2[770](r = +i)$ and $N = 5$ $(r = +i)$ orbitals. If this assignment is adopted for band 2, we must conclude that this structure is observed in a spin range $I = 46-68$, which again exceeds the experimental estimate [11] by $8\hbar$.

According to CRMF calculations, an alternative configuration for band 1 can also be suggested. This is the TSD3(c) configuration obtained from TSD3(a) by particle-hole excitations of two neutrons, see Fig. 2(b). Although TSD3(c) somewhat underestimates experimental $J^{(2)}$, in a spin range of $I = 34-66$ this configuration has $Q_t = 11 - 10.4$ eb that is closer to experiment. In addition, the comparison of theoretical and experimental energies in Fig. 4 suggests that this configuration is consistent with the spin range of $I = 29-71$, which is closer to experimental estimates.

The problem with this interpretation is that TSD3(c) is never predicted very close to yrast (see Fig. 1). While the excitation energy of this configuration is relatively low in CRMF-NL3*, it is substantially larger in CRMF-NL1. It is interesting to note, however, that shifting the neutron $N = 5$ level – from which the associated particle-hole excitations are made – by roughly 1 MeV in NL3* results in a lowering of TSD3(c) so that it becomes competitive with TSD3(a) in the range of $I = 60 - 70$. The analysis of the deformed single-particle states at normal deformations [27] indicates that such a possibility cannot be excluded.

Similar results have also been obtained in our CSHF-SkM* calculations. Since the corresponding shell structure is slightly different as compared to CRMF-NL3* and CRMF-NL1, the energetics of TSD3 bands predicted in CSHF is altered. For example, the lowest TSD3 configuration predicted in CSHF is TSD3(b); it was labeled "D" in Ref. [20]. This configuration can be assigned to band 1. The configuration TSD3(a) is excited by $\sim$1 MeV with respect of TSD3(b). As seen in Fig. 3(b), the dynamic moment of inertia of TSD3(b) above the low-frequency band crossing is lower than that of experimental band 1 and $J^{(2)}$ of CRMF TSD3(b). The latter maybe due to the particular choice of SkM* functional but the different treatment of time-odd mean fields in the CSHF and CRMF [33, 34] is also likely to contribute. The dynamic moments of inertia of TSD3(b) in CSHF shows an unpaired band crossing at $\Omega_x \sim 0.73$ MeV, which is absent in experiment. However, this should not prevent us from assigning band 1 to TSD3(b) since the crossing frequencies strongly depend on relative energies of participating levels, which are not very accurately described in DFT [27, 35, 36]. A similar effect is also seen in the CRMF-NL3* and CRMF-NL1 results for TSD3(b) in Fig. 3(a), which predict a high-frequency unpaired band crossings at frequencies which differ by as much as 0.1 MeV. As discussed in Ref. [20], the calculated transition quadrupole moment $Q_t = 10.7$ eb of TSD3(b) is close to experiment. The comparison between experimental and calculated energies in Fig. 4 indicates that band 1 would have to be observed in the spin range of $I = 31-73$ if TSD3(b) were assigned to this band in CSHF.

In CSHF, band 2 is assigned to TSD3(d) – a configuration built from TSD3(b) by promoting one neutron from the $[N = 5](r = -i)$ routhian into $1/2[651](r = +)$. The dynamic moment of inertia of this configuration is lower than the experimental one and the transition quadrupole moment of this configuration is $Q_t \sim 10.6$ eb. The corresponding $\gamma-$deformation of this configuration is $\sim 11^\circ$. If this configuration assignment is adopted, band 2 should be observed in spin range $I = 44 - 66$, which again is higher than experimental estimates of Ref. [11].

If experimental spin assignments ($I = 23-65$) are used for band 1, then – according to Fig. 4 – only the AX, TSD1, and TSD2 structures of Fig. 1 can be considered as possible candidates for the observed band. However, the transition quadrupole moments predicted for AX and TSD1 are too small to explain experimental data. The results of Ref. [20] indicate that TSD2, which is predicted higher in energy in CSHF, is unphysical. This is consistent with the situation seen in Figs. 1(b) and (c). However, in CRMF-NL3* variant of Fig. 1(a) we find a TSD2 band that competes in energy with TSD1 up to $I \approx 62$. Here, a possibility that TSD2 represents a physical structure – a scenario advocated in Ref. [21] – cannot be ruled out.

In summary, properties of triaxial superdeformed bands at ultra-high spin in ^{158}Er have been analyzed in the framework of relativistic and non-relativistic DFT. The results obtained in these two theoretical frame-

works are consistent. In particular, experimental transition quadrupole moments Q_t and dynamic moments of inertia are well described by TSD3 ($\pi 6^2 \nu 7^1$) configurations having large quadrupole moments and positive $\gamma \approx 10 - 15^\circ$. The calculated spin assignments associated with these bands substantially exceed experimental estimates, which are still subject to large uncertainties. On the other hand, configurations which agree with experimental angular momentum assignments significantly underestimate dynamic moments of inertia and transition quadrupole moments. If the theoretical spins assignments of Fig. 4 turned out to be correct, the experimental band 1 in ^{158}Er would be the the highest-spin structure ever observed. The current study stresses the need for more precise measurements of Q_t and reliable estimates of spins in these bands.

Useful discussions with J. Dobaczewski, I. Ragnarsson, M. A. Riley, R. V. F. Janssens and F. Xu are gratefully acknowledged. This work has been supported by the U. S. Department of Energy under Contracts Nos. DE-FG02-07ER41459 (Mississippi State University) and DE-FG02-96ER40963 (University of Tennessee), and by the Natural Science Foundation of China under Grant No. 10975006.

[1] A. Bohr, Mat. Fys. Medd. K. Dan. Vidensk. Selsk. **26**, no. 14 (1952).

[2] D. L. Hill and J. A. Wheeler, Phys. Rev. **89**, 1102 (1953).

[3] P. Möller, R. Bengtsson, B. G. Carlsson, P. Olivius, T. Ichikawa, H. Sagawa, and A. Iwamoto, At. Data Nucl. Data Tables **94**, 758 (2008).

[4] Z. Szymański, *Fast Nuclear Rotation*, (Clarendon Press, Oxford 1983).

[5] A. V. Afanasjev, D. B. Fossan, G. J. Lane, and I. Ragnarsson, Phys. Rep. **322**, 1 (1999).

[6] R. Wadsworth, R. M. Clark, J. A. Cameron, D. B. Fossan, I. M. Hibbert, V. P. Janzen, R. Krücken, G. J. Lane, I. Y. Lee, A. O. Macchiavelli, C. M. Parry, J. M. Sears, J. F. Smith, A. V. Afanasjev, and I. Ragnarsson, Phys. Rev. Lett. **80**, 1174 (1998).

[7] A. Bohr and B. R. Mottelson, *Nuclear Structure* (Benjamin, New York, 1975), Vol. II.

[8] D. R. Jensen, G. B. Hagemann, I. Hamamoto, S. W. Ødegård, B. Herskind, G. Sletten, J. N. Wilson, K. Spohr, H. Hübel, P. Bringel, A. Neußer, G. Schönwaßer, A. K. Singh, W. C. Ma, H. Amro, A. Bracco, S. Leoni, G. Benzoni, A. Maj, C. M. Petrache, G. Lo Bianco, P. Bednarczyk, and D. Curien, Phys. Rev. Lett. **89**, 142503 (2002).

[9] S. Frauendorf, Rev. Mod. Phys. **73**, 463 (2001).

[10] K. Lagergren, B. Cederwall, T. Bäck, R. Wyss, E. Ideguchi, A. Johnson, A. Ataç, A. Axelsson, F. Azaiez, A. Bracco, J. Cederkäll, Zs. Dombrádi, C. Fahlander, A. Gadea, B. Million, C. M. Petrache, C. Rossi-Alvarez, J. A. Sampson, D. Sohler, and M. Weiszflog, Phys. Rev. Lett. **87**, 022502 (2001).

[11] E. S. Paul, P. J. Twin, A. O. Evans, A. Pipidis, M. A. Riley, J. Simpson, D. E. Appelbe, D. B. Campbell, P. T. W. Choy, R. M. Clark, M. Cromaz, P. Fallon, A. Görgen,D. T. Joss, I. Y. Lee, A. O. Macchiavelli, P. J. Nolan, D. Ward, and I. Ragnarsson, Phys. Rev. Lett. **98**, 012501 (2007).

[12] X. Wang, M. A. Riley, J. Simpson, E. S. Paul, R. V. F. Janssens, A. D. Ayangeakaa, H. C. Boston, M. P. Carpenter, C. J. Chiara, U. Garg, P. Hampson, D. J. Hartley, C. R. Hoffman, D. S. Judson, F. G. Kondev, T. Lauritsen, N. M. Lumley, J. Matta, S. Miller, P. J. Nolan, J. Ollier, M. Petri, D. C. Radford, J. M. Rees, J. P. Revill, L. L. Riedinger, S. V. Rigby, C. Unsworth, S. Zhu, and I. Ragnarsson, Proc. of Rutherford Centennial Conference, in press.

[13] J. Ollier, J. Simpson, X. Wang, M. A. Riley, A. Aguilar, C. Teal, E. S. Paul, P. J. Nolan, M. Petri, S. V. Rigby, J. Thomson, C. Unsworth, M. P. Carpenter, R. V. F. Janssens, F. G. Kondev, T. Lauritsen, S. Zhu, D. J. Hartley, I. G. Darby, andI. Ragnarsson, Phys. Rev. C **80**, 064322 (2009).

[14] M. Mustafa, J. Ollier, J. Simpson, M. A. Riley, E. S. Paul, X. Wang, A. Aguilar, M. P. Carpenter, I. G. Darby, D. J. Hartley, R. V. F. Janssens, F. G. Kondev, T. Lauritsen, P. J. Nolan, M. Petri, J. M. Rees, J. P. Revill, S. V. Rigby, C. Teal, J. Thomson, C. Unsworth, S. Zhu, B. G. Carlsson, H. L. Ma, T. Mufti, and I. Ragnarsson, Phys. Rev. C **84**, 054320 (2011).

[15] J. Ollier, J. Simpson, M. A. Riley, E. S. Paul, X. Wang, A. Aguilar, M. P. Carpenter, I. G. Darby, D. J. Hartley, R. V. F. Janssens, F. G. Kondev, T. Lauritsen, P. J. Nolan, M. Petri, J. M. Rees, S. V. Rigby, C. Teal, J. Thomson, C. Unsworth, S. Zhu, A. Kardan, and I. Ragnarsson, Phys. Rev. C **83** , 044309 (2011).

[16] A. Aguilar, D. B. Campbell, K. Chandler, A. Pipidis, M. A. Riley, C. Teal, J. Simpson, D. J. Hartley, F. G. Kondev, R. M. Clark, M. Cromaz, P. Fallon, I. Y. Lee, A. O. Macchiavelli, and I. Ragnarsson, Phys. Rev. C **77**, 021302(R) (2008).

[17] T. Bengtsson and I. Ragnarsson, Phys. Scr. T5, 165 (1983).

[18] J. Dudek and W. Nazarewicz, Phys. Rev. C 31, 298 (1985).

[19] X. Wang, M. A. Riley, J. Simpson, E. S. Paul, J. Ollier, R. V. F. Janssens, A. D. Ayangeakaa, H. C. Boston, M. P. Carpenter, C. J. Chiara, U. Garg, D. J. Hartley, D. S. Judson, F. G. Kondev, T. Lauritsen, N. M. Lumley, J. Matta, P. J. Nolan, M. Petri, J. P. Revill, L. L. Riedinger, S. V. Rigby, C. Unsworth, S. Zhu, I. Ragnarsson, Phys. Lett. **B702**, 127 (2011).

[20] Yue Shi, J. Dobaczewski, S. Frauendorf, W. Nazarewicz, J. C. Pei, F. R. Xu, and N. Nikolov, Phys. Rev. Lett. 108, 092501 (2012).

[21] A. Kardan, I. Ragnarsson, H. Miri-Hakimabad, and L. Rafat-Motevali, Phys. Rev. **86**, 014309 (2012).

[22] D. Vretenar, A. V. Afanasjev, G. A. Lalazissis, and P. Ring, Phys. Rep. **409**, 101 (2005).

[23] M. Bender, P.-H. Heenen, and P.-G. Reinhard, Rev. Mod. Phys. **75**, 121 (2003).

[24] A. V. Afanasjev, J. König and P. Ring Nucl. Phys. **A608**, 107 (1996).

[25] P.-G. Reinhard, M. Rufa, J. Maruhn, W. Greiner and J. Friedrich, Z. Phys. **A323**, 13 (1986).

[26] G. A. Lalazissis, S. Karatzikos, R. Fossion, D. Peña Arteaga, A. V. Afanasjev, and P. Ring, Phys. Lett. **B671**, 36 (2009).

[27] A. V. Afanasjev and S. Shawaqfeh, Phys. Lett. **B706**, 177 (2011).

[28] N. Schunck, J. Dobaczewski, J. McDonnell, W. Satula, G. A. Sheikh, A. Staszczak, M. Stoitsov, P. Toivanen, Comput. Phys. Commun. **183**, 166 (2012).

[29] J. Bartel, P. Quentin, M. Brack, C. Guet, and H.-B. Hakansson, Nucl. Phys. **A386**, 79 (1982).

[30] A. V. Afanasjev, G. A. Lalazissis, P. Ring, Nucl. Phys. **A634**, 395 (1998).

[31] M. Riley, private communication 2012.

[32] T. Lauritsen, M. P. Carpenter, P. Fallon, B. Herskind, R. V. F. Janssens, D. G. Jenkins, T. L. Khoo, F. G. Kondev, A. Lopez-Martens, A. O. Macchiavelli, D. Ward, K. S. Abu Saleem, I. Ahmad, R. Clark, M. Cromaz, J. P. Greene, F. Hannachi, A. M. Heinz, A. Korichi, G. Lane, C. J. Lister, P. Reiter, D. Seweryniak, S. Siem, R. C. Vondrasek, I. Wiedenhäver, Phys. Rev. Lett. 88, 042501 (2002).

[33] J. Dobaczewski and J. Dudek, Phys. Rev. **C52**, 1827 (1995).

[34] A. V. Afanasjev and H. Abusara, Phys. Rev. **C82**, 034329 (2010).

[35] N. Schunck, J. Dobaczewski, J. McDonnell, J. More, W. Nazarewicz, J. Sarich, and M. V. Stoitsov, Phys. Rev. **C81**, 024316 (2010).

[36] A. V. Afanasjev and S. Frauendorf, Phys. Rev. C **72**, 031301(R) (2005).